catalysts

MDPI

Article

Photocatalytic Removal of Methyl Orange Azo Dye with Simultaneous Hydrogen Production Using Ru-modified ZnO Photocatalyst

Vincenzo Vaiano and Giuseppina Iervolino*

Department of Industrial Engineering, University of Salerno, Via Giovanni Paolo II, 132 Fisciano (Salerno), Italy; vvaiano@unisa.it

* Correspondence: giiervolino@unisa.it

Received: 21 October 2019; Accepted: 13 November 2019; Published: 15 November 2019

Abstract: The aim of this work is to demonstrate the effectiveness of the photocatalytic process in the Methyl Orange azo dye degradation and simultaneous H_2 production by using ZnO doped with ruthenium. Ru-modified ZnO photocatalysts were prepared by precipitation method and were characterized by different techniques (XRF, Raman, XRD, N2 adsorption at −196 °C, and UV–vis DRS). The experiments were carried out in a pyrex cylindrical reactor equipped with a nitrogen distributor device and irradiated by four UV lamps with the main wavelength emission at 365 nm. Different Ru amounts (from 0.10 to 0.50 mol%) were tested in order to establish the optimal amount of the metal to be used for the ZnO doping. The photocatalytic activity was evaluated both in terms of Methyl Orange removal and hydrogen production. The experimental results showed that the best activity, both in terms of H_2 production and Methyl Orange degradation, was obtained with the Ru-modified ZnO photocatalyst at 0.25 mol% Ru loading. In particular, after four hours of UV irradiation time, the discoloration and mineralization degree were equal to 83% and 78%, with a simultaneous hydrogen production of 1216 μmol L^{-1}. This result demonstrates the ability of the photocatalytic process to valorize a dye present in wastewater, managing to obtain a hydrogen production comparable with the data present in the literature today in the presence of other sacrificial substances.

Keywords: photocatalysis; zinc oxide; azo dye; hydrogen production; textile wastewater

1. Introduction

Renewable energies represent the future of our planet. Oil, coal, methane and natural fossil fuels formed during the evolution of the Earth, to date, meet more than 80% of the world's energy needs. However, in relatively short timeframes these resources will come very close to exhaustion. Therefore, scientific research has begun to pay close attention to the efficiency of industrial processes and the minimization of waste, especially in the energy sector. H_2 could be a promising choice for a future energy resource because it is free of pollution, storable, and highly demanded by fuel cell industries. Different technologies have been proposed for its production and photocatalysis represents an innovative technology with wide margins of development. Hydrogen produced via photocatalytic water splitting has been considered as a promising alternative technology [1]. However, the introduction of "sacrificial agents", such as ethanol, methanol, and glucose promotes the photocatalytic hydrogen production [2,3]. The addition of these organic compounds can improve the photocatalytic H_2 production efficiency by consuming the photo-induced hole for better electron–hole separation. At the same time, the concern of the industry is the disposal and treatment of wastewater. In particular, in industrial wastewater, there are many persistent contaminants that can damage the environment and the health of living beings. An interesting approach is to explore the

possibility of producing an energy source, such as hydrogen, in parallel to wastewater treatment, from the degradation of organic substances present in wastewater through the photocatalytic application [4]. In fact, if the sacrificial agent is a pollutant present in water or wastewater, the overall process would enhance the H_2 production rate while simultaneously degrading the organic substrate [5]. Nowadays, much attention has been paid to the huge amount of dye-containing wastewater generated by the textile industry. The presence of coloured effluents causes both a negative aesthetic impact, but also serious environmental pollution. Organic dyes are one of the most serious water pollutants, due to their high production volumes from industry, toxicity, and low biodegradability [6]. It has been estimated that the annual production of organic dyes amounts to approximately one million tons and a significant amount (about 10–15%) of wastewater containing dyes is discharged to the surface water without any treatment [7]. Some organic dyes are carcinogenic to humans and negatively affect aquatic organisms by interfering with their metabolic processes [8]. Textile dyes with complex structures are highly resistant to conventional physicochemical and biological degradation. In order to obtain the removal of these kinds of pollutants, advanced oxidation processes have been studied. Much progress has been made in the field of photocatalytic processes for the removal of textile dyes [9–12]. Therefore, it could be interesting to exploit the capabilities of photocatalysis to convert this type of organic pollutant into compounds with high added value. In literature, the use of bifunctional TiO_2 photocatalysts, achieved through the surface modification of TiO_2 with metal nanoparticles or two different components, has been proposed for simultaneous hydrogen production and pollutant degradation (urea) in the presence of UV light [13]. Titania is one of the most widely used semiconductors in heterogeneous photocatalysis, both for the removal of pollutants from wastewater [14], and for hydrogen production via water splitting (Miyoshi et al., 2018) or reforming of organic substances [15]. An aqueous solution containing an azo dye, Acid Orange 7 (initial concentration: 12 mg/L), and a Pt/TiO_2 photocatalyst irradiated by UV light, was used to combine into a single process the dye degradation and hydrogen production [5]. In this paper, a photocatalytic hydrogen production equal to about 4000 μmol/L, after 8 hours of irradiation, was observed [5]. In literature, the simultaneous production of molecular hydrogen and degradation of rhodamine B (RhB) was reported [6]. In this case, TiO_2 modified with platinum and nafion ($Pt/TiO_2/Nf$) under visible light ($\lambda > 420$ nm) was used. This photocatalyst exhibited high activity for H_2 production in the presence of an RhB dye pollutant and ethylenediaminetetraacetic acid (EDTA), which act as a photosensitizer and an electron donor, respectively. With an initial concentration of RhB equal to 10 mg/L and EDTA equal to 4 mM, approximately 2300 μmol/L of H_2 was produced after 14 hours of visible light irradiation [6]. In another paper, photocatalytic hydrogen production was performed by a visible-light-driven ternary photocatalyst, zinc oxysulfide ($ZnO_{0.6}S_{0.4}$), in the presence of a sulfide/sulfite (S^{2-}/SO_3^{2-}) sacrificing system, with simultaneous azo-dye Reactive Violet 5 (RV5) degradation [16]. Results of other studies using different photocatalysts and dye pollutants are listed in Table 1.

Table 1. Comparison of hydrogen production from the data of other literature with different photocatalysts.

Photocatalyst (Co-Catalyst)	Sacrificing Agent	Light Source*	H_2 Production Rate ($\mu mol\ g^{-1}\ h^{-1}$)	Reference
ZnO0.6S0.4	Sulfide/sulfite + RV5	Vis	49.2	[16]
Ti^{3+}-doped TiO_2 (1% Pt)	Methylene Blue	Vis	~14	[17]
Ti^{3+}-doped TiO_2 (1% Pt)	Rhodamine B	Vis	~8.3	[17]
Ti^{3+}-doped TiO_2 (1% Pt)	Methyl Orange	Vis	~5	[17]
TiO_2 (0.5% Pt)	Methanol + Methyl Orange	UV–vis	~420	[18]
Simonkolleite–TiO_2	Remazole Red	UV–vis	~825	[19]
TiO_2 (0.5% Pt)	Acid Orange 7	UV–vis	~450	[5]
$Pt/TiO_2/Nf$	RhB dye pollutant + EDTA	UV	~380	[6]

It is not easy to compare the data from different literature because the experimental conditions are different, such as the photocatalyst dosage, the type of dye, the presence of co-catalysts, the light source, and so on. However, it is interesting to collect literature data on this topic to understand the interest of the scientific community and the developments. As observed in Table 1, the most

commonly used photocatalyst in this field is TiO_2. However, in addition to TiO_2, several semiconductors, such as ZnO [20] and $LaFeO_3$ [21] have been proposed in the literature, whose performances seem to be competitive compared to those of TiO_2. Among these photocatalysts, it is well known that ZnO is an environment-friendly semiconductor with a bandgap of 3.37 eV. However, the quick recombination of the photoexcited electrons and holes in ZnO always leads to a decline in the photocatalytic efficiency [22]. It is possible to solve this problem by applying modifications to the electronic structure of the catalyst, for example by modifying the surface of the semiconductor with the addition of other elements, such as metals, metal oxides, or through a synergistic effect in combination with another semiconductor. In this way, it is possible to improve the efficiency of the photocatalyst in these reactions [23]. Besides noble metals, transition metals can also be used to dope the semiconductors, improving the trapping of electrons and inhibiting the electron–hole recombination. In particular, ruthenium, a transition metal, is much cheaper than noble metals (about eight times less expensive than rhodium;) but it is shown to be able to improve the photocatalytic efficiency of the semiconducting materials in the same way. For example, the performances of Ru/CeO_2 catalysts in the catalytic wet air oxidation of acrylic, succinic acids have been reported [24]. Aranganayagam et al. showed the photocatalytic activity of Ru-modified ZnO for the removal of an azo dye in an aqueous solution [25]. From the photocatalytic results the authors evidenced that Ru-modified ZnO has a photocatalytic property better than pure ZnO. Therefore, considering the performance of the ZnO photocatalyst and the properties of the transition metals effective for the semiconductor modifications, the aim of this work was to demonstrate the effectiveness of a Ru-modified ZnO photocatalyst for the degradation of a textile azo dye, Methyl Orange (MO), with the simultaneous H_2 production under UV irradiation.

2. Results and Discussion

2.1. Characterizations and Results

The XRD results of the undoped and Ru-modified ZnO, with different Ru contents, are reported in Figure 1. From the spectra, in the range 20–80°, it is possible to observe the main peaks at 31.90°, 34.58°, 36.43°, 47.08°, and 56.72°, typical of the hexagonal wurtzite crystal structure, respectively indexed to the (1 0 0), (0 0 2), (1 0 1), (1 0 2), and (1 1 0) planes [26]. The addition of Ru did not induce changes in the crystalline structure of ZnO. This last result is consistent with the literature concerning Ru-modified ZnO [27]. In addition, no signals related to metallic Ru or ruthenium oxides were observed for 0.1 and 0.25 Ru mol%. On the other hand, as doping percentage of Ru was increased up to 0.5 mol%, a very weak signal at about 39° corresponding to RuO_2 appeared [28].

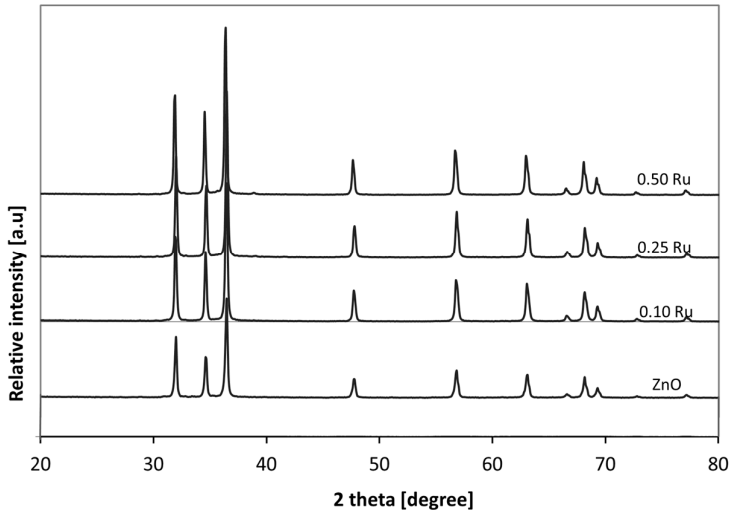

Figure 1. XRD spectra of undoped ZnO and Ru-modified ZnO photocatalysts in the range 20–80°.

The average crystallite size (calculated using the Scherrer equation [29]) of the bare ZnO was 35 nm (Table 2). With an increase of the Ru amount up to 0.25 mol%, the crystallite size decreased to 32 nm, but when the Ru content was further increased to 0.5 mol%, the value of crystallite size slightly increased, being equal to 33 nm (Table 2). Accordingly, the highest SSA value was observed for the 0.25 Ru photocatalyst (Table 2).

Table 2. The chemical-physical characteristics of the prepared photocatalysts.

Photocatalyst	Ru Nominal Amount [%mol]	Ru Measured* Amount [%mol]	Band Gap Energy** [eV]	Crystallite Size [nm]	SSA** [m²/g]
ZnO	0	0	3.20	35	5.5
0.10Ru	0.10	0.09	3.20	34	6.1
0.25Ru	0.25	0.22	3.20	32	7.2
0.50Ru	0.5	0.53	3.17	33	5.8

* by XRF analysis; ** by UV–vis diffuse reflectance spectroscopy (DRS), *** by Brunauer, Emmett and Teller method (B.E.T.).

The results of Raman analysis in the range of 200–700 cm^{-1} of the all prepared catalysts are shown in Figure 2. The main band at 438 cm^{-1} corresponds to the non-polar optical phonons E_2 (high) mode of ZnO [30]. At 583 cm^{-1} Raman shift there is the signal probably attributed to the longitudinal optical phonon (LO) feature, due to the formation of defects such as oxygen vacancy, as reported in the literature [31].

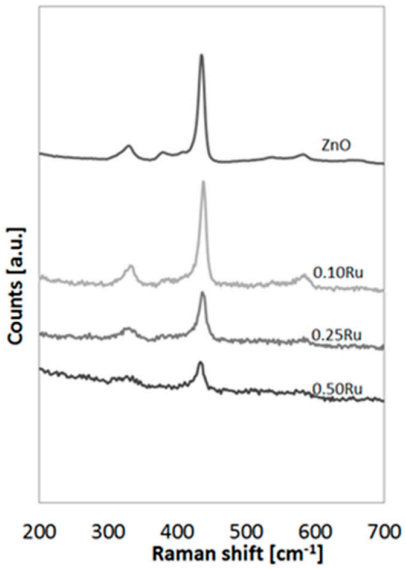

Figure 2. Raman spectra of the undoped and Ru-modified ZnO in the range 200–700 cm^{-1}.

It was observed that, as the Ru doping concentration was increased, the intensities of the spectra decreased and the LO feature signal tended to disappear [32]. Optical absorption properties of the catalysts were studied through UV–vis DRS in the range of 300–900 nm (Figure 3). The undoped zinc oxide presents the typical reflectance spectrum of UV active semiconducting materials, with the absorption onset at about 390 nm. After the doping of the ZnO with Ru, an improvement in the intensity of light absorption in the UV region was observed. All the Ru-modified ZnO samples evidenced a continuous absorption in the visible range and the absorption was stronger with the increase of Ru content [27]. This last result may be explained considering the fact that undoped ZnO appears as a white powder, while the modification with ruthenium turns the samples into dark green colour, which is more pronounced at a higher Ru concentration [33]. Some authors associate this

phenomenon to the excitation of the electrons from the valance band of ZnO to the unoccupied level of the metal cluster [34]. However, the presence of the Ru doping did not affect the band gap energy value of the prepared photocatalysts. A slight decrease in the band gap value is obtained only in the case of the higher ruthenium molar percentage used for the doping (0.50 mol%). Thus, the beneficial effect of Ru may be related to its ability to act as an efficient electron trap, thereby preventing the electron–hole recombination. The results of the band gap energy are reported in Table 2.

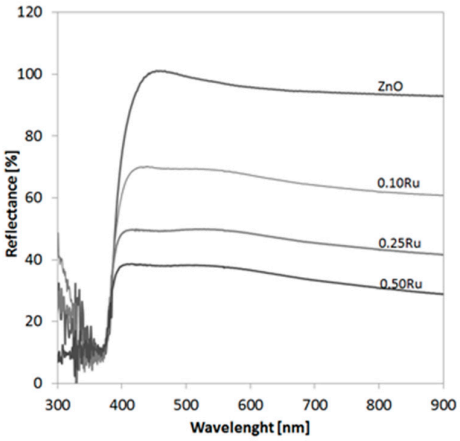

Figure 3. UV–Vis DRS spectra of undoped and Ru-modified ZnO photocatalyst in terms of reflectance as a function of wavelength.

2.2. Photocatalytic Activity Results

The effect of Ru content on photocatalytic H_2 production and MO removal are reported in Figure 4 and Figure 5a,b, respectively. All the Ru-modified ZnO photocatalysts demonstrated a photoactivity better than the undoped ZnO. The greatest hydrogen production (1216 μmol L^{-1}) was achieved for the 0.25 Ru catalyst after 4 h of UV irradiation time (Figure 4). The hydrogen production efficiency increased when Ru mol% was increased from 0.10 to 0.25 mol% and decreased when the Ru content was further increased up to 0.50 mol%, reaching a value equal to 983 μmol L^{-1} after 4 h of irradiation time. In terms of MO degradation, the results obtained with different Ru content showed very similar discoloration and mineralization values (about 82% and 78% of discoloration and mineralization at the end of the test, respectively) (Figure 5a,b). Aiming to obtain, simultaneously, the degradation of the azo dye and its valorization in terms of hydrogen production, the optimal catalyst must be considered the 0.25 Ru sample. These results are very interesting if compared with the literature data [18].

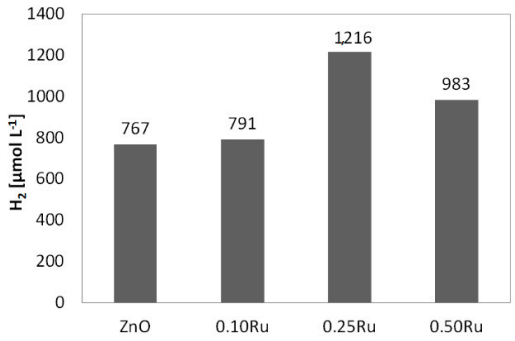

Figure 4. Effect of Ru content on H_2 production after 4 h of UV irradiation time.

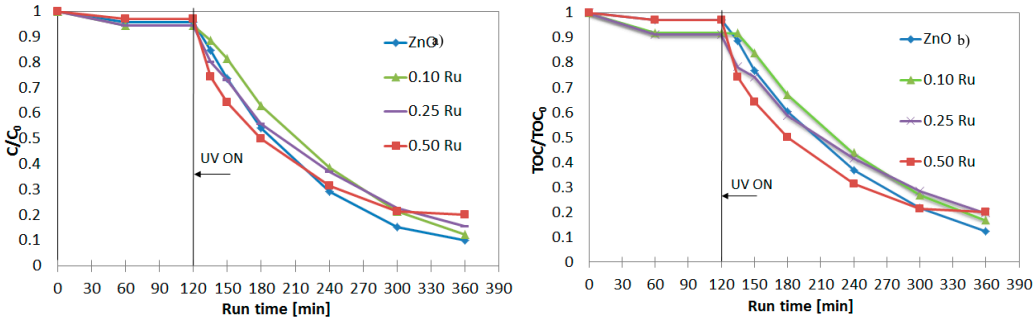

Figure 5. Effect of the Ru content on methyl orange (MO) discoloration (**a**) and mineralization (**b**) during the run time.

In literature, it has been reported that the photocatalytic hydrogen production from MO (at 20 mg L^{-1} initial concentration) degradation is improved by methanol addition (2.5 M) and using a Pt based photocatalyst [18]. In this last case, the maximum hydrogen production was equal to about 9 μmol g^{-1}_{cat} min^{-1}. In our case, the highest hydrogen production corresponds to about 1 μmol g^{-1}_{cat} min^{-1}. Although this production seems much lower than that found in the literature, it must be considered that, in our case, the hydrogen production was obtained in the absence of an additional sacrificial agent (methanol) and noble metals. Moreover, in the present study it is possible to assume that the MO degradation occurs thanks to the photogenerated oxygen from the water oxidation under UV irradiation. According to the literature [5], it is possible to argue that the photogenerated oxygen is consumed for the oxidation of the MO until its complete mineralization is obtained. The effect of catalyst dosage on the performances of the system after 4 h of UV irradiation was also evaluated (Figure 6). The photocatalytic efficiency increased as the catalyst loading was increased up to 1.5 g L^{-1}. Further increase of catalyst load resulted in a decrease of hydrogen production (Figure 6). The presence of an optimal value for the catalyst loading is likely related to the limiting effect of the interception of the light by the catalyst particles on the degradation efficiency [35]. Moreover, from the experimental results, a correlation between the dye percentage adsorbed in dark conditions on the catalyst surface and the hydrogen production obtained during the UV irradiation has emerged. The exposed catalyst surface area decreases as the catalyst dosage increases due to aggregation phenomena of photocatalyst particles [36], worsening the amount of the adsorbed dye. This last parameter also influences the photocatalytic hydrogen production. In fact, the highest percentage of MO adsorbed (obtained with a catalyst dosage equal to 1.5 g L^{-1}) corresponds to the highest hydrogen production (Figure 6).

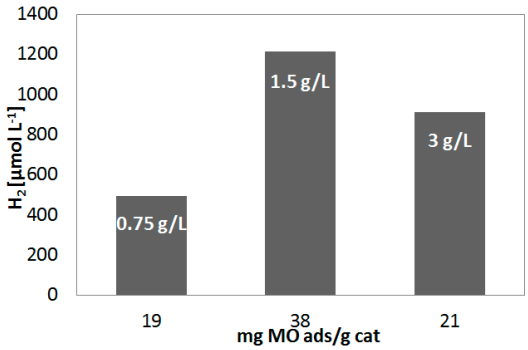

Figure 6. The effect of catalyst dosage on H_2 production after 4 h of UV irradiation time.

Photocatalytic hydrogen production obtained following the addition of variable concentrations of MO (in the range 5–20 mg L^{-1}) to the solution prior to exposure to light, at the spontaneous pH, are summarized in Figure 7. The results evidence that an optimal initial concentration of dye exists and

with this concentration the highest hydrogen production was obtained. This behaviour is in agreement with the literature about the photocatalytic hydrogen production from azo dyes in an aqueous solution [5].

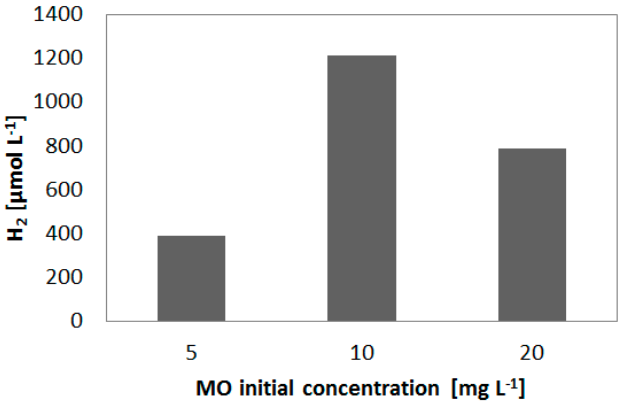

Figure 7. Effect of MO initial concentration on H_2 production after 4 h of UV irradiation time.

It is observed that the addition of a small amount of dye (from 5 to 10 mg L^{-1}) results in significantly enhanced H_2 production (from 387 to 1216 μmol L^{-1}) after 4 h of UV irradiation. Further increase of MO initial concentration up to 20 mg L^{-1} does not result in the enhancement of hydrogen production (equal to 790 μmol L^{-1}), at least during the irradiation time period of the experiment (4 h), indicating that longer irradiation times are probably necessary for this case [5].

3. Materials and Methods

3.1. Photocatalysts Preparation and Characterization

Ru-modified ZnO photocatalysts were prepared by a precipitation method. An undoped ZnO photocatalyst was prepared using 5 g of zinc acetate dihydrate $ZnC_4H_6O_4$ (Sigma Aldrich, 99%) as precursor salt, dissolved in 50 mL of distilled water. A NaOH (Sigma Aldrich, 99%) aqueous solution (obtained dissolving 2 g of NaOH in 25 mL of distilled water) was slowly added in order to obtain a precipitate. The obtained precipitate compounds were centrifuged, washed with distilled water, and calcined at a temperature equal to 600 °C for 2 h. Beforehand, in the case of Ru-modified ZnO, different amounts of $RuCl_3$ (Sigma Aldrich, 99%) (Table 2) were added to the solution of $ZnC_4H_6O_4$ to cause precipitation by the addition of NaOH. The obtained precipitate was centrifuged, washed, and calcined at 600 °C for 2 h. The Ru nominal amount is expressed as a molar percentage and it was calculated through Equation (1).

$$\%\text{mol Ru} = \frac{n\,Ru}{n\,Ru + n\,Zn} \times 100, \quad (1)$$

Where n Ru is the number of moles of $RuCl_3$ used in the synthesis and n Zn is the number of moles of $ZnC_4H_6O_4$ used in the synthesis. The prepared photocatalysts were characterized with several techniques. In particular, the Raman spectra of the samples were realized with a Dispersive MicroRaman system (Invia, Renishaw, England), equipped with 514 nm laser, in the range 100–2000 cm^{-1} Raman shift. Total Ru content of the samples was evaluated by X-ray fluorescence spectrometry (XRF) in a thermos Fischer ARL QUANT'X EDXRF spectrometer (Italy) equipped with a rhodium standard tube as the source of the radiation and with a Si-Li drifted crystal detector. XRD analysis was carried out to evaluate the crystal phases of the prepared photocatalysts by a Brucker D8 diffractometer, with a scan rate equal to 0.05 °/second (analysis range in the range 20–80 degrees). UV–vis reflectance spectra (UV–vis DRS) of powder catalysts were measured by a Perkin Elmer spectrometer (Italy) Lambda 35 using a reflectance spectroscopy accessory (Labsphere Inc., North

Sutton, NH, United States of America). The photocatalysts band gap was determined from Kubelka–Munk function $F(R\infty)$ by plotting $[F(R\infty) \times h\nu]^2$ vs. $h\nu$. The specific surface areas (SSA) of the photocatalysts were evaluated through Brunauer-Emmett-Teller (B.E.T.) method by N_2 adsorption at −196 °C with a Costech Sorptometer 1042 after a pretreatment at 150 °C for 1 h in a He flow.

3.2. Photocatalytic Experiments

The photocatalytic experiments were performed with a Pyrex reactor with a cylindrical configuration (ID = 2.5 cm) equipped with a N_2 distributor device (Q = 0.125 NL min^{-1}). Irradiation was provided by four UV lamps (Philips, the nominal power was 8 W and the main peak of emission was 365 nm) positioned around the external surface of the reactor at an equal distance from it (about 0.5 cm) in order to uniformly irradiate the volume of the suspension. During the tests a specific amount of catalyst was suspended in 80 mL of an aqueous solution with methyl orange azo dye (MO) at 10 mg L^{-1} initial concentration (pH = 6.3). Different catalyst dosages (0.75, 1.5, and 3 g L^{-1}) were tested. The solution to be treated is continuously mixed by a peristaltic pump. The photocatalytic experiment is characterized by a first dark phase, necessary to reach the adsorption and desorption equilibrium of the MO on the catalyst surface, and by a second phase lasting 4 hours in the presence of UV light. The analysis of the gaseous phase from the photoreactor (city, State Abbr. (if has), country) was realized by continuous H_2 analysers (ABB Advance Optima). About 2 mL of the aqueous sample was taken from the photoreactor at different times and centrifuged in order to remove photocatalyst particles before the analyses. The MO concentration was measured by a spectrophotometric method at λ = 462 nm (Perkin Elmer spectrophotometer, Italy).

4. Conclusions

The results of this work demonstrate the effectiveness of the Ru-modified ZnO photocatalyst in the simultaneous degradation and valorization of organic contaminants, such as Methyl Orange azo dye, present in aqueous solutions. Undoped and Ru-modified ZnO photocatalysts, with different Ru content, were successfully synthesized by a simple precipitation method. XRD and Raman analysis showed the presence of the characteristic ZnO signals, while from UV–vis DRS results it was evidenced that the doping of ZnO with Ru enhances the intensity of the light absorption in the UV region, but has no significant effect on the band gap value. Moreover, a correlation between the amount of adsorbed dye on the catalyst surface and the hydrogen production during heterogeneous photocatalysis was observed. The optimal Ru content was equal to 0.25 mol% and from the photocatalytic results the obtained hydrogen production was equal to 1216 μmol L^{-1} after 4 h of UV irradiation time. This was higher than that obtained with undoped ZnO (767 μmol L^{-1}). This result was very interesting since it showed the possibility of using the photocatalytic process not only for the degradation of azo dyes present in wastewater, but also the possibility of converting these organic substances into high added value compounds (such as H_2).

Author Contributions: G.I. performed the experiments and wrote the manuscript. V.V. provided the concept and experimental design of the study and reviewed the paper prior to submission. Both the authors discussed the results, analyzed the data, and commented on the manuscript.

Funding: This research received no external funding

Acknowledgement: The authors wish to thank Eng. Immacolata Sansone for the support in the photocatalytic tests.

Conflicts of Interest: The authors declare no conflict of interest.

References

1. Liao, C.-H.; Huang, C.-W.; Wu, J. Hydrogen production from semiconductor-based photocatalysis via water splitting. *Catalysts* **2012**, *2*, 490–516.
2. Iervolino, G.; Vaiano, V.; Sannino, D.; Rizzo, L.; Ciambelli, P. Photocatalytic conversion of glucose to H_2 over $LaFeO_3$ perovskite nanoparticles. *Chem. Eng. Trans.* **2016**, *47*, 283–288.

3. Christoforidis, K.C.; Fornasiero, P. Photocatalytic hydrogen production: A rift into the future energy supply. *ChemCatChem* **2017**, *9*, 1523–1544.
4. Iervolino, G.; Vaiano, V.; Sannino, D.; Rizzo, L.; Palma, V. Enhanced photocatalytic hydrogen production from glucose aqueous matrices on Ru-doped $LaFeO_3$. *Appl. Catal. B Environ.* **2017**, *207*, 182–194.
5. Patsoura, A.; Kondarides, D.I.; Verykios, X.E. Enhancement of photoinduced hydrogen production from irradiated Pt/TiO_2 suspensions with simultaneous degradation of azo-dyes. *Appl. Catal. B Environ.* **2006**, *64*, 171–179.
6. Kim, J.; Park, Y.; Park, H. Solar hydrogen production coupled with the degradation of a dye pollutant using TiO_2 modified with platinum and nafion. *Int. J. Photoenergy* **2014**, *2014*, 324859.
7. Gupta, V. Application of low-cost adsorbents for dye removal—A review. *J. Environ. Manag.* **2009**, *90*, 2313–2342.
8. Crini, G. Non-conventional low-cost adsorbents for dye removal: A review. *Bioresour. Technol.* **2006**, *97*, 1061–1085.
9. Vaiano, V.; Iervolino, G. Facile method to immobilize ZnO particles on glass spheres for the photocatalytic treatment of tannery wastewater. *J. Colloid Interface Sci.* **2018**, *518*, 192–199.
10. Somasundaram, S.; Veerakumar, P.; Lin, K.C.; Kumaravel, V. Application of nanocomposites for photocatalytic removal of dye contaminants. *Photocatal. Funct. Mater. Environ. Remediat.* **2019**, 131–161, doi:10.1002/9781119529941.ch4.
11. Bouras, H.D.; Isik, Z.; Arikan, E.B.; Bouras, N.; Chergui, A.; Yatmaz, H.C.; Dizge, N. Photocatalytic oxidation of azo dye solutions by impregnation of ZnO on fungi. *Biochem. Eng. J.* **2019**, *146*, 150–159.
12. Zuorro, A.; Lavecchia, R.; Monaco, M.M.; Iervolino, G.; Vaiano, V. Photocatalytic degradation of azo dye reactive violet 5 on Fe-doped titania catalysts under visible light irradiation. *Catalysts* **2019**, *9*, 645.
13. Kim, J.; Monllor-Satoca, D.; Choi, W. Simultaneous production of hydrogen with the degradation of organic pollutants using TiO_2 photocatalyst modified with dual surface components. *Energy Environ. Sci.* **2012**, *5*, 7647–7656.
14. He, Y.; Sutton, N.B.; Rijnaarts, H.H.; Langenhoff, A.A. Degradation of pharmaceuticals in wastewater using immobilized TiO_2 photocatalysis under simulated solar irradiation. *Appl. Catal. B Environ.* **2016**, *182*, 132–141.
15. Bahruji, H.; Bowker, M.; Davies, P.R.; Pedrono, F. New insights into the mechanism of photocatalytic reforming on Pd/TiO_2. *Appl. Catal. B Environ.* **2011**, *107*, 205–209.
16. Chu, K.H.; Ye, L.; Wang, W.; Wu, D.; Chan, D.K.L.; Zeng, C.; Yip, H.Y.; Jimmy, C.Y.; Wong, P.K. Enhanced photocatalytic hydrogen production from aqueous sulfide/sulfite solution by $ZnO_{0.6}S_{0.4}$ with simultaneous dye degradation under visible-light irradiation. *Chemosphere* **2017**, *183*, 219–228.
17. Wang, J.; Zhang, P.; Li, X.; Zhu, J.; Li, H. Synchronical pollutant degradation and H_2 production on a Ti^{3+}-doped TiO_2 visible photocatalyst with dominant (0 0 1) facets. *Appl. Catal. B Environ.* **2013**, *134*, 198–204.
18. Romão, J.; Salata, R.; Park, S.-Y.; Mul, G. Photocatalytic methanol assisted production of hydrogen with simultaneous degradation of methyl orange. *Appl. Catal. A Gen.* **2016**, *518*, 206–212.
19. Badawy, M.I.; Ali, M.E.; Ghaly, M.Y.; El-Missiry, M.A. Mesoporous simonkolleite—TiO_2 nanostructured composite for simultaneous photocatalytic hydrogen production and dye decontamination. *Process Saf. Environ. Prot.* **2015**, *94*, 11–17.
20. Vaiano, V.; Jaramillo-Paez, C.A.; Matarangolo, M.; Navío, J.A.; del Carmen Hidalgo, M. UV and visible-light driven photocatalytic removal of caffeine using ZnO modified with different noble metals (Pt, Ag and Au). *Mater. Res. Bull.* **2019**, *112*, 251–260.
21. Tijare, S.N.; Joshi, M.V.; Padole, P.S.; Mangrulkar, P.A.; Rayalu, S.S.; Labhsetwar, N.K. Photocatalytic hydrogen generation through water splitting on nano-crystalline $LaFeO_3$ perovskite. *Int. J. Hydrogen Energy* **2012**, *37*, 10451–10456.
22. Xie, M.-Y.; Su, K.-Y.; Peng, X.-Y.; Wu, R.-J.; Chavali, M.; Chang, W.-C. Hydrogen production by photocatalytic water-splitting on Pt-doped TiO_2–ZnO under visible light. *J. Taiwan Inst. Chem. Eng.* **2017**, *70*, 161–167.
23. Chen, X.; Lou, Y.; Dayal, S.; Qiu, X.; Krolicki, R.; Burda, C.; Zhao, C.; Becker, J. Doped semiconductor nanomaterials. *J. Nanosci. Nanotechnol.* **2005**, *5*, 1408–1420.
24. Ibhadon, A.; Greenway, G.; Yue, Y. Photocatalytic activity of surface modified $TiO_2/RuO_2/SiO_2$ nanoparticles for azo-dye degradation. *Catal. Commun.* **2008**, *9*, 153–157.

25. Aranganayagam, K.; Senthilkumaar, S.; Ganapathi Subramaniam, N.; Kang, T.W. Ruthenium doped ZnO semiconductor: Synthesis, characterization and photodegradation of azo dye. *Int. J. Nanosci.* **2013**, *12*, 1350009.
26. Yayapao, O.; Thongtem, T.; Phuruangrat, A.; Thongtem, S. Synthesis and characterization of highly efficient Gd doped ZnO photocatalyst irradiated with ultraviolet and visible radiations. *Mater. Sci. Semicond. Process.* **2015**, *39*, 786–792.
27. Manríquez, M.E.; Noreña, L.E.; Wang, J.A.; Chen, L.; Salmones, J.; González-García, J.; Reza, C.; Tzompantzi, F.; Hernández Cortez, J.G.; Ye, L. One-pot synthesis of Ru-doped ZnO oxides for photodegradation of 4-chlorophenol. *Int. J. Photoenergy* **2018**, *2018*, 7605306.
28. Reksten, A.H.; Russell, A.E.; Richardson, P.W.; Thompson, S.J.; Mathisen, K.; Seland, F.; Sunde, S. Strategies for the analysis of the elemental metal fraction of Ir and Ru oxides via XRD, XANES, and EXAFS. *Phys. Chem. Chem. Phys.* **2019**, *21*, 12217–12230.
29. Wojnarowicz, J.; Mukhovskyi, R.; Pietrzykowska, E.; Kusnieruk, S.; Mizeracki, J.; Lojkowski, W. Microwave solvothermal synthesis and characterization of manganese-doped ZnO nanoparticles. *Beilstein J. Nanotechnol.* **2016**, *7*, 721–732.
30. Zhang, Q.; Liu, J.-K.; Wang, J.-D.; Luo, H.-X.; Lu, Y.; Yang, X.-H. Atmospheric self-induction synthesis and enhanced visible light photocatalytic performance of Fe^{3+} doped Ag-ZnO mesocrystals. *Ind. Eng. Chem. Res.* **2014**, *53*, 13236–13246.
31. Janotti, A.; Van de Walle, C.G. Fundamentals of zinc oxide as a semiconductor. *Rep. Progress Phys.* **2009**, *72*, 126501.
32. Ilanchezhiyan, P.; Kumar, G.M.; Subramanian, M.; Jayavel, R. Effect of Pr doping on the structural and optical properties of ZnO nanorods. *Mater. Sci. Eng. B* **2010**, *175*, 238–242.
33. Bloh, J.Z.; Dillert, R.; Bahnemann, D.W. Ruthenium-modified zinc oxide, a highly active vis-photocatalyst: The nature and reactivity of photoactive centres. *Phys. Chem. Chem. Phys.* **2014**, *16*, 5833–5845.
34. Sakthivel, S.; Shankar, M.; Palanichamy, M.; Arabindoo, B.; Bahnemann, D.; Murugesan, V. Enhancement of photocatalytic activity by metal deposition: Characterisation and photonic efficiency of Pt, Au and Pd deposited on TiO_2 catalyst. *Water Res.* **2004**, *38*, 3001–3008.
35. Chakrabarti, S.; Dutta, B.K. Photocatalytic degradation of model textile dyes in wastewater using ZnO as semiconductor catalyst. *J. Hazard. Mater.* **2004**, *112*, 269–278.
36. Mohagheghian, A.; Karimi, S.-A.; Yang, J.-K.; Shirzad-Siboni, M. Photocatalytic degradation of a textile dye by illuminated tungsten oxide nanopowder. *J. Adv. Oxid. Technol.* **2015**, *18*, 61–68.